ELSEVIER

Materials Science and Engineering A309–310 (2001) 270–273

MATERIALS SCIENCE & ENGINEERING A

www.elsevier.com/locate/msea

# Kinetic Monte Carlo modeling of dislocation motion in BCC metals

Wei Cai [a,*], Vasily V. Bulatov [b], Sidney Yip [a], Ali S. Argon [a]

[a] *Department of Nuclear Engineering, Massachusetts Institute of Technology, Cambridge, MA 02139, USA*
[b] *Lawrence Livermore National Laboratory, University of California, Livermore, CA 94550, USA*

**Abstract**

We present a kinetic Monte Carlo (kMC) simulation method for modeling screw dislocation motion in BCC metals on the micron–second scales, using inputs from atomistic simulations of core mechanisms on the angstrom–picosecond scale. The simulations use atomistic input such as double-kink nucleation energy and kink mobility, include linear elastic (Peach–Koehler) interactions between dislocation segments, and predict overall dislocation velocity at different temperature and stress states. In addition, an important mechanism, namely, the spontaneous superjog growth and debris loop nucleation, is identified in the kMC simulation as an important factor controlling the dislocation motion in the high stress and medium temperature regime. 

*Keywords:* Dislocation; Kinetic Monte Carlo; BCC metals

## 1. Introduction

Dislocation velocity as a function of stress and temperature is the single most important material input for large-scale dislocation dynamics (DD) simulations [1]. In principle, dislocation motion is controlled by core mechanisms which should and can be examined on an atomistic level. While molecular dynamics (MD) and other atomistic modeling approaches can reproduce the dynamics of dislocation behavior in all relevant details, only relatively small dislocation segments can be modeled because so much details are followed, and then only on picosecond–nanosecond time scales. We propose a mesoscopic approach to predicting dislocation motion on the μm/second scale in BCC metals, based on atomic core mechanisms, in a kinetic Monte Carlo (kMC) implementation.

KMC simulations have previously been applied successfully by the authors to model dislocation motion in Si [2–4] as a net result of multiple elementary processes such as double-kink nucleations and kink migrations, all taking place simultaneously. In this paper, we will focus on the differences in implementation and the outcome of such mesoscopic simulations in BCC metals (using Mo as a prototype) and those in Si. One particular aspect that we explore in this paper is the consequences of easy cross-slip in BCC metals by which the motion of screw dislocations becomes three-dimensional. This is in contrast to two-dimensional nature of dislocation motion in Si, where even screw dislocations are confined to glide in the dissociation planes and cross-slip events are rare.

Our kMC simulations show that, in the high stress and medium temperature regime, as a direct consequence of cross-slip, a moving screw dislocation can initiate spontaneous self-pinning and subsequent kink pile-ups, which can eventually lead to debris dislocation loop formation. While this process arises naturally in our simulations under certain stress and temperature conditions, it has been proposed before as the hardening mechanism for Ti-Al [5]. Below we discuss this mechanism and its effects on the screw dislocation mobility in BCC metals.

## 2. Simulation methodology

In the present model, we study a screw dislocation represented by a piece-wise straight line stretched along the $1/2\langle 1\,1\,1\rangle$ Burgers vector, as shown in Fig. 1. The dislocation line consists of horizontal (H) and vertical (V) segments, with H-segments being pure screw and V-segments being pure edge, representing kinks. V-segments all have the same length $h$, the unit kink height, while H-segments can be of any length. This edge-screw representation of a dislocation is similar to edge-screw discretization employed in some DD simulations [1], although the edge segments are used there for a different purpose, i.e. to represent continuously curved dislocation lines.

In our model kink pairs are allowed to nucleate on any part of H-segments and in any of the three $\{1\,1\,0\}$ glide planes $a$, $b$ and $c$ intersecting the $\langle 1\,1\,1\rangle$ direction. Once nucleated,

* Corresponding author.
*E-mail address:* caiwei@mit.edu (W. Cai).

0921-5093/01/$ – see front matter 
PII: S0921-5093(00)01689-0

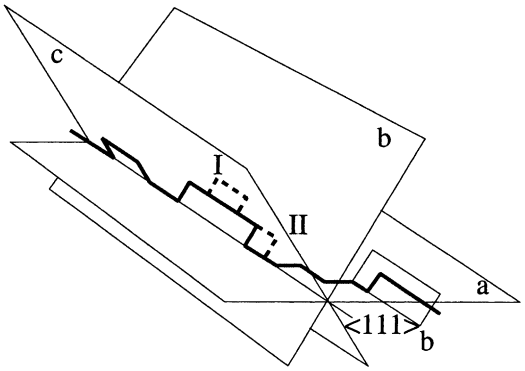


Fig. 1. Schematic representation of dislocation in BCC metals in the kMC simulation. The dislocation line is mostly aligned along the $1/2\langle 1\,1\,1\rangle$ Burgers vector. Double-kinks can nucleate on either of the three $\{1\,1\,0\}$ planes *a*, *b* and *c*, while kink migration is constrained on its own glide plane. A double-kink nucleation event is shown at position, I, and a kink migration event is shown at position II, both in dashed lines.

a kink (V-segment) can move in its glide plane along the dislocation line until it recombines with another kink with the opposite sign. Periodic boundary conditions are applied so that kinks leaving at one end re-enter the dislocation from the other end. During kMC simulations, the dislocation moves under the action of external stress through kink pair nucleation, migration and recombination. A description of the simulation methodology is given below.

Atomistic simulations using empirical many-body potential MGPT [6] have calculated kink pair nucleation energy barrier on screw dislocations in Mo to be 2 eV, in the absence of external stress. While no similar atomistic data are available under finite stress and at finite temperatures, Edagawa's line tension model [7] provides a reasonable description of variations of the double-kink nucleation energy as a function of loading stress. Combining Edagawa's model with the atomistic data [6], we calculated and tabulated the double-kink nucleation enthalpy $H_{\mathrm{dk}}$ as a function of the magnitude $\tau$ of the shear stress and the angle $\chi$ between the maximum resolved shear stress (MRSS) plane and the glide plane. A simple functional form for $H_{\mathrm{dk}}(\tau, \chi)$ was then fitted to the tabulated values and subsequently used for calculating the rate of kink pair nucleation events per lattice site, as given by the standard transition state theory [8] formula,

$$j_{\mathrm{dk}} = \omega_0 \exp\left(-\frac{H_{\mathrm{dk}}(\tau, \chi)}{k_B T}\right) \tag{1}$$

where $\omega_0$ is an attempt frequency factor, and is set equal to the *Debye frequency* of Mo in this work. The fact that the nucleation rate given by Eq. (1) only depends on the magnitude and the direction of the MRSS is the result of the approximations made in the Edagawa's line tension model — some possible non-Schmid effects are ignored.

In contrast to high Peierls barrier for kink pair nucleation, kink motion on screw dislocations in Mo is extremely easy, as manifested in the low kink (or secondary) Peierls barrier ($\sim$0.0005 eV), given by atomistic calculations [9] using an embedded atom method empirical potential. Such a low energy barrier means that kink migration along the screw dislocation is not thermally activated but is controlled by the phonon drag mechanism. Because the kinks on a screw dislocation can be viewed as short edge segments, their high mobility is consistent with recent MD simulations of edge dislocations motion [10] in Mo using the same potential. We have also carried out a series of MD simulations of similar type to study the motion of screw dislocations containing a single kink. According to our preliminary results [11], the drag coefficient for kink motion is $B = 4.5 \times 10^{-5}$ Pa s. Consequently, in the present kMC simulations, the kink velocity is calculated as

$$v_{\mathrm{k}} = \frac{\tau_{\mathrm{g}} b}{B} \tag{2}$$

where $\tau_{\mathrm{g}}$ is the glide component of the resolved shear stress and $b$ the Burgers vector.

Now we present a brief description of our kMC simulation algorithm.

1. At the beginning of each kMC step, stress is calculated along the entire dislocation line, which determines double-kink nucleation rate on H-segments and kink velocity of V-segments through Eqs. (1) and (2), respectively.
2. Assuming that all the kinks move with constant velocity calculated at this moment, a migration time $t_{\mathrm{mig}}$ is then computed as the upper limit of the time before any kink has moved more than a prescribed distance, and before any kink pair annihilation or debris dislocation loop formation (see below).
3. A nucleation time $t_{\mathrm{nuc}}$ is generated as a random number from the exponential distribution defined by the total nucleation rate. The latter is calculated by summing up kink pair nucleation rates on all H-segments.
4. If $t_{\mathrm{mig}} < t_{\mathrm{nuc}}$, then all kinks move with the current velocity for a time period $t_{\mathrm{mig}}$. If any kink pair recombination or debris loop formation events are detected, they are carried out and the algorithm returns to step 1. Otherwise, the kinks move with their current velocities for a time period $t_{\mathrm{nuc}}$, followed by a kink pair nucleation on an H-segment. The nucleation site is chosen according to the local nucleation rates by a standard kMC algorithm [3]. Return to 1.

We now discuss the mechanism of "debris dislocation loop" formation mentioned in step 2 above. The process starts when two kink pairs form spontaneously on two different $\{1\,1\,0\}$ planes, due to the easy cross-slip. As illustrated in Fig. 2(a), when two of such cross kinks move towards each other and collide, they cannot recombine. Because they are pushed towards each other by external stress the kinks are now constrained to move together. In such cases, the forces on the two cross kinks act in the opposite directions along the line and the cross kinks can slow down or halt their coupled motion altogether. Such elementary kink-jog (or cross kinks) pairs grow in size when more kinks pile-up on

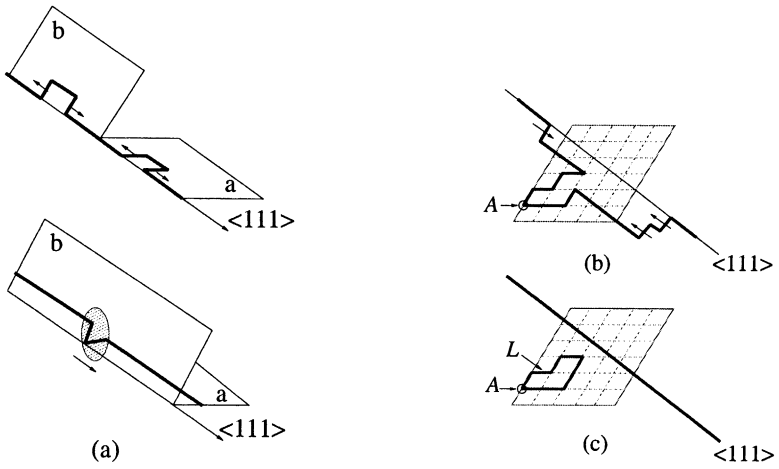


Fig. 2. Schematic representation of the formation of (a) two kinks forming an elementary superjog (or cross-kink), (b) more kinks joining the superjog, and (c) debris loop $L$ formation with the primary dislocation breaking away from the self-pinning point A.

either sides of the initial pinning point (A) forming superjogs [12], as shown in Fig. 2(b). Again, due to the easy cross-slip, the kinks in the pile-ups on two sides of the pinning point may belong to different planes. Consequently, projections of the two developing pile-ups on the $\langle 1\,1\,1\rangle$ plane appear similar to two random walk trajectories originating from the same point (initial cross kink) on a two-dimensional lattice. If and when two such trajectories cross each other, the dislocation line may reconnect by recombination of kink pairs. As a result, the two pile-ups are now reduced in size leaving behind a prismatic (debris) loop $L$, shown in Fig. 2(c).

## 3. Results

Fig. 3 shows two snapshots of kMC simulations of screw dislocation motion at 373 K under 320 MPa shear stress with different orientations of the MRSS plane. In these plots, the H-segments are significantly shrunken compared to the V-segments in order to show the entire dislocation line; the total length of the H-segments are in fact 27 μm while each V-segment is only 2.5 Å. In Fig. 3(a), the MRSS plane bisects two glide planes $a$ and $b$, making kink pair nucleation equally probable on both planes. Cross-kinks and debris loops are readily observed in this case. In Fig. 3(b), the MRSS plane is parallel to glide plane $b$ and double-kinks mostly nucleate on this plane. In addition, the resolved shear stress on the glide plane $b$ is much larger than that in the previous case, resulting in a much higher kink density. The choice of such a moderately high stress and temperature values in these two simulations is to maintain enough number of kinks on the dislocation. At low stress and low temperatures, the simulation results become rather trivial, in that there is always only one kink pair along

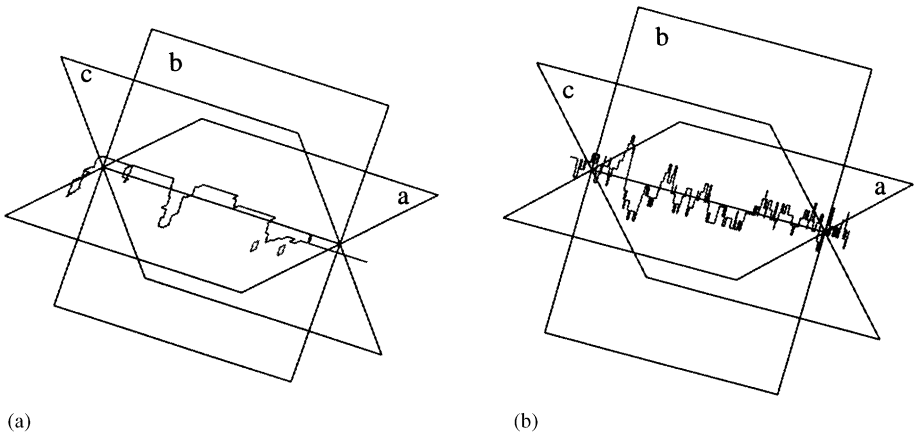


Fig. 3. Snapshots of kMC simulations of screw dislocation motion at 373 K under 320 MPa resolved shear stress with different orientations. The H-segments are significant shrunken compared to the V-segments in order to show the entire dislocation line; the total length of the H-segments are in fact 27 μm while each V-segment is only 2.5 Å. (a) MRSS plane bisects the glide plane $a$ and $b$, making double-kink nucleations equally probable on the two planes. Superjogs and debris loops are readily observed. (b) MRSS plane is parallel to glide plane, $b$, and double-kinks mostly nucleate on this plane. The resolved shear stress on the glide plane is much larger resulting in a much higher kink density.

the entire dislocation line. In this case, the dislocation mobility is probably controlled by other mechanism such as forest obstacles instead of by self-pinning and superjog growth.

As in our earlier simulations [2], we monitor the instantaneous average dislocation position as a function of time and obtain dislocation velocity from the slope. We find that different orientations of the MRSS plane lead to distinctly different behaviors of moving dislocations and, consequently, to different dislocation mobilities. In case (a), the averaged double-kink nucleation rate per lattice site on plane $a$ is $j_{dk} = 1.5 \times 10^5 b^{-1}\,s^{-1}$, and the averaged kink velocity is $v_k = 6.2 \times 10^{12} b\,s^{-1}$, where $b$ is the Burgers vector. The overall dislocation velocity along plane $a$ is found to be $v = 6.8\,cm\,s^{-1}$, which would be about half of what the kink diffusion model of Hirth and Lothe would predict [13], $v_{HL} = \sqrt{2}h(Jv_k)^{1/2} = 11\,cm\,s^{-1}$. On the other hand, in case (b), $j_{dk} = 1.3 \times 10^7 b^{-1}\,s^{-1}$, $v_k = 7.1 \times 10^{12} b\,s^{-1}$, dislocation velocity of $v = 343\,cm\,s^{-1}$ obtained in the kMC simulation is in agreement with the kink diffusion model prediction of $v_{HL} = 349\,cm\,s^{-1}$. The reason for such a considerable difference between the two models in the case (a) is that, in our model, spreading of kink pairs is constrained by pile-ups formed at cross kinks. In the presence of such pinning points many kink pairs eventually recombine with themselves and do not contribute to the overall dislocation motion.

## 4. Concluding remarks

We have developed a kMC approach for modeling dislocation motion in BCC metals at the scale of multiple microns. We find that in the high stress and medium temperature regime, easy cross-slip of screw dislocations can result in self-pinning, superjog growth and several other mechanisms whose competition controls the motion of screw dislocations in BCC metals. Our model predicts variations in dislocation velocities with stress and temperature that can be directly compared with experimental measurements [14,15].

## Acknowledgements

W. Cai and S. Yip acknowledge support from the Lawrence Livermore National Laboratory under an ASCI-level 2 program. V.V. Bulatov acknowledges support from the Office of Basic Energy Sciences, the US Department of Energy. We thank Dr. L. Kubin for many helpful discussions.

## References

[1] M. Tang, L.P. Kubin, G.R. Canova, Acta Mater. 9 (1998) 3221.
[2] W. Cai, V.V. Bulatov, J.F. Justo, S. Yip, A.S. Argon, Phys. Rev. Lett. 84 (2000) 3346.
[3] W. Cai, V.V. Bulatov, S. Yip, J. Comput.-Aided Mater. Design 6 (2/3) (1999) 175–183.
[4] W. Cai, V.V. Bulatov, J.F. Justo, S. Yip, A.S. Argon, Mater. Res. Soc. Proc. 538 (1999) 69.
[5] F. Louchet, B. Viguier, Philos. Mag. A. 80 (2000) 765.
[6] W. Xu, J. Moriarty, Comput. Mater. Sci. 9 (1998) 348.
[7] K. Edagawa, T. Suzuki, S. Takeuchi, Phys. Rev. B. 55 (1997) 6180.
[8] S. Glasstone, K.J. Laidler, H. Eyring, The Theory of Rate Processes, McGraw-Hill, New York, NY, 1941.
[9] J. Moriarty, M.S. Duesbery, private communication.
[10] J. Chang, V.V. Bulatov, S. Yip, J. Comput.-Aided Mater. Design 6 (2/3) (1999) 165–173.
[11] W. Cai, unpublished data.
[12] J.P. Hirth J. Lothe, Theory of Dislocations, Wiley, New York, 1982, p. 261.
[13] J.P. Hirth J. Lothe, Theory of Dislocations, Wiley, New York, 1982, p. 545.
[14] E.B. Leiko, E.M. Nadgornyi, Kristallografiya 19 (1974) 584.
[15] E.B. Leiko, D.V. Lotsko, E.M. Nadgornyi, V.I. Trefilov, Sov. Phys. Solid State 17 (1975) 1814.